Automated Blood Vessel Extraction Based on High-Order Local Autocorrelation Features on Retinal Images

Yuji Hatanaka[1(✉)], Kazuki Samo[2], Kazunori Ogohara[1], Wataru Sunayama[1], Chisako Muramatsu[3], Susumu Okumura[4], and Hiroshi Fujita[3]

[1] Department of Electronic Systems Engineering, School of Engineering, The University of Shiga Prefecture, Hikone, Japan
hatanaka.y@e.usp.ac.jp
[2] Division of Electronic Systems Engineering, Graduate School of Engineering, The University of Shiga Prefecture, Hikone, Japan
[3] Department of Intelligent Image Information, Graduate School of Medicine, Gifu University, Gifu, Japan
[4] Department of Mechanical Systems Engineering, School of Engineering, The University of Shiga Prefecture, Hikone, Japan

Abstract. Automated blood vessels detection on retinal images is an important process in the development of pathologies analysis systems. This paper describes about an automated blood vessel extraction using high-order local autocorrelation (HLAC) on retinal images. Although HLAC features are shift-invariant, HLAC features are weak to turned image. Therefore, a method was improved by the addition of HLAC features to a polar transformed image. We have proposed a method using HLAC, pixel-based-features and three filters. However, we have not investigated about feature selection and machine learning method. Therefore, this paper discusses about effective features and machine learning method. We tested eight methods by extension of HLAC features, addition of 4 kinds of pixel-based features, difference of preprocessing techniques, and 3 kinds of machine learning methods. Machine learning methods are general artificial neural network (ANN), a network using two ANNs, and Boosting algorithm. As a result, our already proposed method was the best. When the method was tested by using "Digital Retinal Images for Vessel Extraction" (DRIVE) database, the area under the curve (AUC) based on receiver operating characteristics (ROC) analysis was reached to 0.960.

Keywords: Blood vessel extraction · High-order local autocorrelation · Machine learning classifier · Segmentation

1 Introduction

Funduscopy is useful for early detection of diabetic retinopathy, hypertensive retinopathy, arteriosclerotic fundus, and glaucoma. Retinas are examined using retinal images. In most cases, ophthalmologists or physicians use the Scheie classification or

J.M.R.S. Tavares and R.M. Natal Jorge (eds.), *VipIMAGE 2017*,
Lecture Notes in Computational Vision and Biomechanics 27,
DOI 10.1007/978-3-319-68195-5_87

Keith-Wagner classification based on the condition of blood vessels. Hypertensive retinopathy is graded by the diameter ratio of arteries and veins, hemorrhages, and exudates. However, human observation does not provide quantitative results.

Thus, many blood vessel extraction methods have been proposed. Soares et al. proposed a method by classifying each image pixel as vessel or nonvessel, based on the pixel's feature vector composed of the pixel's intensity and two-dimensional Gabor wavelet transform responses taken at multiple scales [1]. Rangayyan et al. proposed a method including the design of a bank of directionally sensitive Gabor filters with tunable scale and elongation parameters [2]. Ricci et al. proposed a method by using two orthogonal line detectors along with the grey level of the target pixel [3]. Staal et al. proposed a method based on image ridge extraction using a k-NN (k nearest neighbor) classifier with properties of the patches and line elements [4].

In general, determining parameters, such as optimal filter size and shape, is difficult. To the best of our knowledge, a blood vessel extraction method based on the relation of neighbor pixels has not been proposed. Ohtsu et al. proposed the use of high-order local autocorrelation (HLAC) features as the primitive image features [5]. HLAC features are shift-invariant and model-free. HLAC is appropriate for center-shifted hotspot pattern feature extraction. A general filtering technique depends strongly on a preset model. Patterns of blood vessels are so varied that designing a flexible blood vessel model is not practical.

We think that HLAC is effective for blood vessel extraction because of HLAC does not require a preset model. Therefore, we have proposed a method using local auto-correlation features, pixel-based-features and three filters [6]. However, we have not investigated about feature selection and machine learning method. The purposed of this study is to discuss about effective features and machine learning method.

2 Materials and Methods

2.1 Database

The retinal images used in this study were obtained from the "Digital Retinal Images for Vessel Extraction" (DRIVE) database [4]. The database includes 40 retinal fundus images that were obtained from a diabetic retinopathy screening program in the Netherlands and are equally divided into training and testing sets. The images were 565 × 584 pixels and 24 bit color. For each image, manual segmentation result for blood vessels is provided as a reference standard.

2.2 HLAC Features

The 0th–2th order HLAC are applied as the feature of blood vessels extraction. The N-th order HLAC is calculated by the following autocorrelations

$$R_N^T(a_1, a_2, \ldots, a_N) = \sum\nolimits_r I(r)I(r+a_1)\ldots I(r+a_N) \tag{1}$$

where $I(r)$ is a pixel value of the image, T is mask pattern number, $r = (x, y)'$ (the dash denotes the transpose) is position vector a, a_i are the displacement vectors, and x and y are coordinates in the image. The top of Fig. 1(a) shows an example when $N = 2$ and $T = 22$. T is limited to 35 ($T = 1, 2, \ldots, 35$) as shown in Fig. 1(b), when the mask size is 3×3 pixels. In this study, 105 mask patterns are defined because of mask size is expanded to 5×5 and 7×7, as shown in Fig. 1(a).

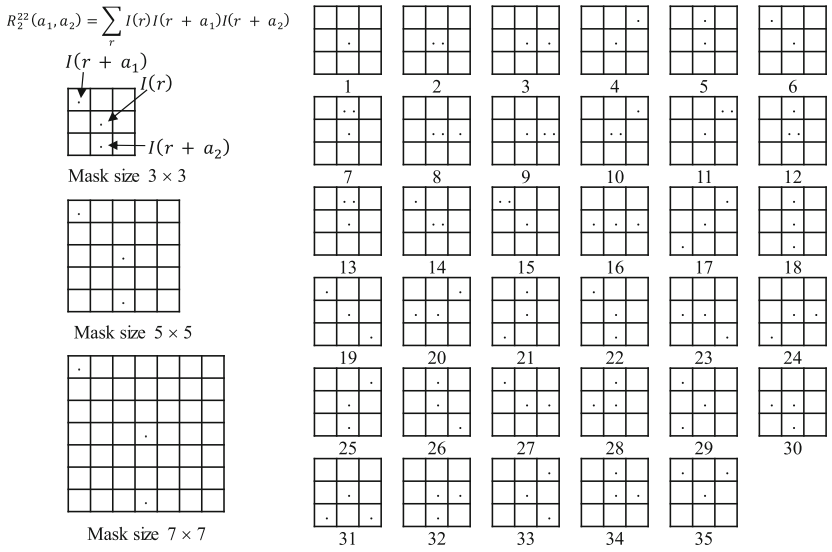

Fig. 1. Local mask patterns for HLAC. (a) Mask pattern corresponding to specific displacement vectors (Pattern No. 22). Middle and bottom windows are extended mask patterns. (b) No. 1 is the 0th order, Nos. 2 to 6 are the first order, and Nos. 7 to 35 are the second order.

HLAC has directional dependency, thus we transformed the ROI to a polar coordinate image and calculated the HLAC as shown in Fig. 2. HLAC features with polar transformation are considered turn-invariant.

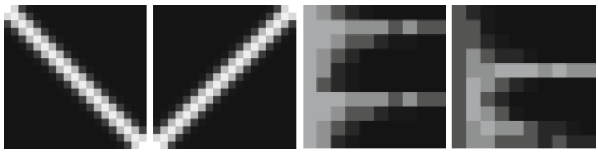

Fig. 2. Polar transformation of ROI: (a) and (b) blood vessel models; (c) and (d) polar-transformed images of (b) and (c).

2.3 Features for Blood Vessels Extraction

The contrast of blood vessels is highest in the green channel of the color retinal image; thus, a grayscale image was obtained using the green channel. Due to the flash, there is an atypical change in the color of the fundus images. Consequently, the grayscale images were preprocessed using γ-correction and histogram-spreading. The blood vessel regions were enhanced by black-top-hat (BTH) transformation as shown in Fig. 3(b) [7]. A 19 × 19-pixel ROI was set in the BTH image, and ROI was converted to 64 gray levels. To ensure rotation invariance, the ROI was then transformed to a 10 × 10-pixel polar coordinate image as shown in Fig. 3. By scanning the retinal images, 105 mask patterns of HLAC features of all pixels were calculated.

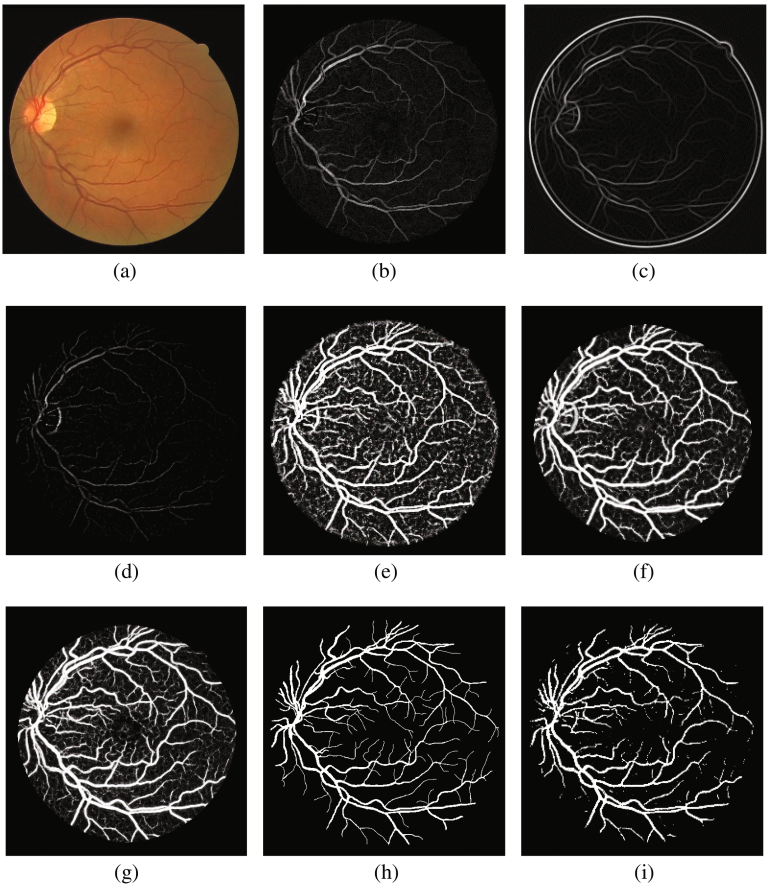

Fig. 3. Examples of blood vessel extraction (image no. 1): (a) original color image; (b) BTH transformation; (c) GF; (d) DR filter; (e) basic HLAC; (f) FANN;(g) SANN; (h) binarized SANN; (i) manual segmentation (ground truth)

Moreover, we prepared four pixel based features and outputs of three filters for blood vessel extraction. Four pixel-based features are the maximum value, minimum value, mean and standard deviation of the green channel pixel values in the ROI. Three filters were BTH transformation, Gabor filter and double-ring filter [8]. Figure 3(b)–(d) show their results.

2.4 D Blood Vessels Extraction Using Classifiers Based on Machine Learning

An artificial neural network (ANN) used in the previous method [6] is showed in Fig. 4. One hundred five HLAC features and four pixel-based features were input to a first ANN (FANN). Moreover, a second ANN (SANN) with five middle layer units classified the blood vessels by using the output of ANN, the green channel pixel values, outputs of three filters. SANN outputs an image as shown in Fig. 3(g). In this study, we also investigated a method based on Boosting with 105 HLAC features, 4 pixel-based features and 3 filter outputs as a classifier candidate.

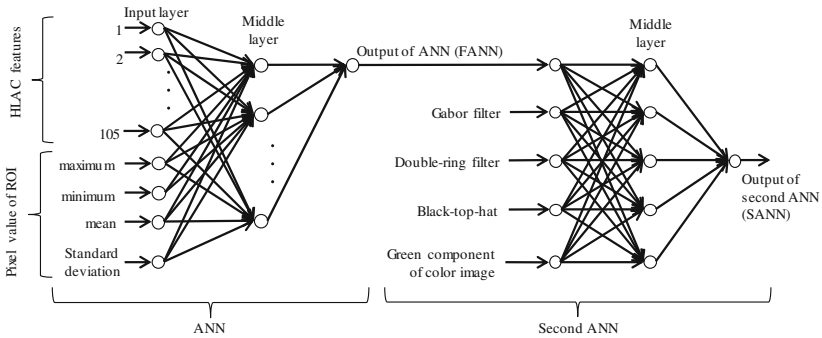

Fig. 4. Two artificial neural networks (ANN). First ANN (FANN) was constructed 12 middle layer units, and it outputs the preliminary blood vessels image. Second ANN (SANN) was constructed by using 5 middle layer unites, and the final blood vessel image is outputted.

3 Results and Discussion

For selection of effective features, we compared performances of six methods by using Area Under the Curve (AUC) based on Receiver Operating Characteristic (ROC). Their results are summarized in Table 1. Six methods were Basic HLAC, HLAC+PBFs, Extended HLAC, BTH+HLAC, FANN and SANN. Basic HLAC classified blood vessels by using ANN with basic 35 HLAC patterns (3×3 window), which were calculated in the green channel images. HLAC+PBFs used Basic HLAC with four pixel-based features (PBFs). Extended HLAC used ANN with 105 HLAC patterns (3×3, 5×5 and 7×7 windows) in the green channel images. BTH HLAC used ANN with basic 35 HLAC patterns in BTH filtered images. FANN was a method based on one ANN by inputting 105 HLAC patterns and PBFs in BTH-filtered images. SANN was the previous method [6].

Table 1. Comparison of performances.

Methods	Features						
	BTH	PBFs	Extended HLAC features	Three filters	Second ANN	AUC	Accuracy
Basic HLAC	–	–	–	–	–	0.918	–
HLAC+PBFs	–	•	–	–	–	0.927	–
Extended HLAC	–	–	•	–	–	0.925	–
BTH+HLAC	•	–	–	–	–	0.921	–
FANN	•	•	•	–	–	0.935	–
SANN	•	•	•	•	•	**0.960**	**0.945**
Boosting FANN	•	•	•	–	–	0.917	–
Boosting SANN	•	•	•	•	–	0.935	–
Soares et al.	Gabor wavelet transform					0.961	0.947
Rangayyan et al.	Gabor filters					0.961	–
Ricci et al.	Two orthogonal line detectors					0.963	0.960
Staal et al.	Image ridge extraction					0.952	0.944
Second human observer						–	0.947

Figure 3(b)–(h) showed results of filtering by using BTH transformation, GF, DR filter, basic HLAC, FANN and SANN. In Fig. 3(b), BTH transform enhanced clear blood vessels, but noise component was conspicuous. GF also enhanced almost blood vessels, but some edges not blood vessels were incorrectly enhanced as shown in Fig. 3(c). DR filter enhanced fat blood vessels although thin blood vessels were not enhanced as shown in Fig. 3(d). Basic HLAC and FANN enhanced clear blood vessels as shown in Fig. 3(e) and (f). FANN could obtain images with less noise components. However, their HLAC output blood vessels wider than them of ground truth. Their HLAC also incorrectly enhanced the border of the optic disc. On the other hand, SANN enhanced almost blood vessels without the border of the optic disc. By applying threshold technique, the image processed by SANN is binarized as shown in Fig. 3(h). On the other hand, SANN enhanced almost blood vessels without the border of the optic disc. By applying threshold technique, the image processed by SANN is binarized as shown in Fig. 3(h). In comparison with the binarized result and the ground truth as shown in Fig. 3(i), they were similar. To discuss about effective features and machine learning method, false positive reduction techniques were not implemented in this study. Therefore, the binarized image as shown in Fig. 3(h) is not optimal.

Table 1 shows that PBFs, 105 HLAC features (Extended HLAC) and BTH were effective. Moreover, two-stage ANN (SANN) was very effective in this test. SANN used three filters. The correlations of HLAC (ANN) and three filters were not high, although HLAC used the output of BTH. Therefore, it is effective to use three filters for SANN.

Then, we tested Boosting algorithm instead of FANN. Boosting is a machine learning algorithms which convert weak learners to strong ones. As a result, the AUC of the Boosting instead of FANN was 0.917. When Boosting was used instead of SANN, the AUC was 0.935. Boosting showed worse performances than FANN and SANN. By applying Boosting algorithm to a data with lots noise components, that tends to show a low performance. There are blood vessels with low contrast in retinal images. Therefore, much noise were incorrectly extracted by using Boosting. We thought that the generalization capability of the Boosting was weak, and overfitting was caused.

By using SANN, the maximum accuracy reached to 0.945. The sensitivity and the specificity were 0.742 and 0.976, respectively. When second observer in DRIVE project segmented blood vessels manually, the sensitivity, the specificity and accuracy were 0.776, 0.973 and 0.947, respectively.

FANN is applied after BTH transformation. In Table 1, two orthogonal line detectors from Ricci et al. shows the best performance. Therefore, if two orthogonal line detectors was applied instead of BTH transformation in FANN, the performance of FANN would be improved. Note that SANN did not include noise reduction algorithm. If noise reduction algorithm added to SANN, the performance would be increased. Therefore, SANN was sufficient performance for blood vessel extraction.

4 Conclusion

We have proposed a blood vessel extraction method using HLAC features, four pixel-based features and three filters based on an ANN. When the performances of seven methods, the AUC of ANN based method reached 0.961. The proposed method can be useful for automatic blood vessel extraction.

Acknowledgments. This research was supported by grants from the Telecommunications Advancement Foundation and JSPS KAKENHI, with grant numbers 16K01415 and 26108005, respectively.

References

1. Soares, J.V., Leandro, J.J., Cesar Júnior, R.M., Jelinek, H.F., Cree, M.J.: Retinal vessel segmentation using the 2-D Gabor wavelet and supervised classification. IEEE Trans. Med. Imaging **25**(9), 1214–1222 (2006)
2. Rangayyan, R.M., Ayres, F.J., Oloumi, F., Oloumi, F., Eshghzadeh-Zanjani, P.: Detection of blood vessels in the retina with multiscale Gabor filters. J. Electron. Imaging **17**(2), 023018 (2008)
3. Ricci, E., Perfetti, R.: Retinal blood vessel segmentation using line operator and support vector classification. IEEE Trans. Med. Imaging **26**(10), 1357–1365 (2007)
4. Staal, J., Abràmoff, M.D., Niemeijer, M., Viergever, M.A., van Ginneken, B.: Ridge based vessel segmentation in color images of the retina. IEEE Trans. Med. Imaging **23**(4), 501–509 (2004)
5. Otsu, N., Kurita, T.: A new scheme for practical, flexible and intelligent vision systems. In: Proceedings of IAPR Workshop on computer Vision, pp. 431–435 (1988)

6. Hatanaka, Y., Samo, K., Tajima, M., Ogohara, K., Muramatsu, C., Okumura, S., Fujita, H.: Automated blood vessel extraction using local features on retinal images. In: Proceedings of SPIE Medical Imaging 2016: Computer-Aided Diagnosis, p. 97852F (2016)
7. Nakagawa, T., Hayashi, Y., Hatanaka, Y., et al.: Recognition of optic nerve head using blood-vessel-erased image and its application to production of simulated stereogram in computer-aided diagnosis system for retinal images. IEICE Trans. Inf. Syst. **J89-D**(11), 2491–2501 (2006)
8. Hatanaka, Y., Nakagawa, T., Zhou, X., Hara, T., Fujita, H., Kakogawa, M., Hayashi, Y., Mizukusa, Y., Fujita, A.: Automated detection algorithm for arteriolar narrowing on fundus images. In: Proceedings of the 27th Annual International Conference of the IEEE Engineering in Medcine and Biology Society, pp. 286–289 (2005)